AMB2025-06 and AMB2025-07 Benchmark Measurements and Challenge Results

Last updated on 12/12/2025

0. Overview

The following describes compiled benchmark challenge measurement results, which are used to judge submissions to the 2025 AM-Bench modeling challenges. The results presented here are summarized and formatted similar to how modelers were asked to submit their modeling results. Additional context, description, or measurement results may also be provided where necessary. Additional information may become available later so updated versions of these documents may be posted. Please check back occasionally. Please note that the measurement results presented here are focused on the challenge problems and reflect only part of the validation measurement data, which will be provided by AM Bench for each set of benchmarks.

1. Challenges

AMB2025-06: Arrays of adjacent laser tracks (pads) on alloy 718 material with two pad geometries and three scenarios: (1) bare plate, no powder layer, (2) 80 µm powder layer on plate, and (3) 160 µm powder layer on plate. Detailed measurement and challenge descriptions are found here (https://www.nist.gov/ambench/am-bench-2025-measurements-and-challenge-problems).

- Pad Melt Pool Geometry (CHAL-AMB2025-06-PMPG): Laser track geometrical measurements (depth, width, etc.) describing the overlapping laser tracks at specified locations of all pads. Additional metrics include the total solidified area above the substrate and the total dilution area below the substrate.
- Pad Surface Topography (CHAL-AMB2025-06-PST): Surface roughness and fused layer thickness measurements for different regions of the pads.

AMB2025-07: Arrays of adjacent laser tracks (pads) on alloy 718 material with two pad geometries and two laser turnaround (i.e., skywriting) times. These experiments used bare plates with no powder. Detailed descriptions are found here (https://www.nist.gov/ambench/am-bench-2025-measurements-and-challenge-problems).

- Pad Cooling Rate and Time Above Melting (CHAL-AMB2025-07-PCRTAM): Cooling rate immediately following complete solidification (below solidus) at specified locations within pads. Time above the midpoint between the solidus and liquidus

temperatures for the melt pool at specified locations within pads. This metric is closely related to melt pool length but is explicitly location specific.

- Pad Melt Pool Geometry (CHAL-AMB2025-07-PMPG): Laser track geometrical measurements (depth, width, etc.) describing the overlapping laser tracks at specified locations of all pads. In addition, the final track melt pool shape for all pads.

Table 1. AMB2025-06 and AMB2025-07 unique variables. Each experiment includes 5 mm × 5 mm and 1 mm × 5 mm pad geometries. Other fixed parameters were the laser power (285 W), laser scan speed (960 mm/s), and laser gaussian diameter (72 µm). The powder and substrate were both nickel superalloy 718.

AM Bench Challenge Number	Laser turnaround times (ms)	Powder Layers (µm)
06	0.75	0 (bare plate), 80, 160
07	0.75, 5.0	0 (bare plate)

2. Results

Results are presented for the four challenge problems associated with AMB2025-06/07. In most cases, results include a standard deviation from repeats. An uncertainty budget will be provided in the future with the dataset(s) and/or publication(s). Please refer to the measurement descriptions document for measurement definitions found here (https://www.nist.gov/ambench/am-bench-2025-measurements-and-challenge-problems).

2.1 CHAL-AMB2025-06-PMPG

Modelers were asked to predict the average melt pool dimensions for the 45 tracks in pads at specific cross-section locations. The cross-section positions are shown in Figure 1. The location names of “edge” and “middle” are used for simplicity to describe a cross-section near the edge of the pad or in the middle of a pad. The positions, listed in tables, were determined with an estimated uncertainty of ± 75 µm (p = 95%). More details on the cross-section positions can be found in the measurement and challenge descriptions document. Figure 2 shows micrographs for the first 7 tracks to illustrate the similarities and differences based on the pad width, cross-section position, and powder layer thickness. For the 1 mm pad width, there is significant remelting back into previous tracks on the surface. The melt pool boundary becomes increasingly difficult to distinguish because there is very little difference in the dendritic microstructure on either side of the boundaries. An example is shown in Figure 3. The boundary that is clear is drawn on and marked as ‘definite’; whereas the portion of the boundary that is not clear is marked as ‘possible’ based on experience and knowledge from other images and experiments. In this

case, the melt pool boundary, and thus bead height and width values, could not be reliably measured. This is reflected by “NA” for some PMPG results.

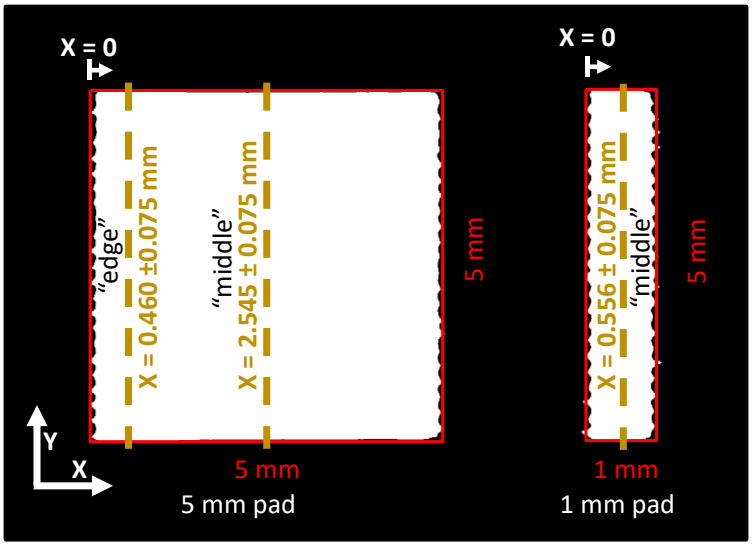

Figure 1. Top view of pads showing cross-section positions: 5 mm pad, edge and middle; 1 mm pad middle. The positions were measured from the left edge of each pad (see measurement and challenge descriptions document for more details).

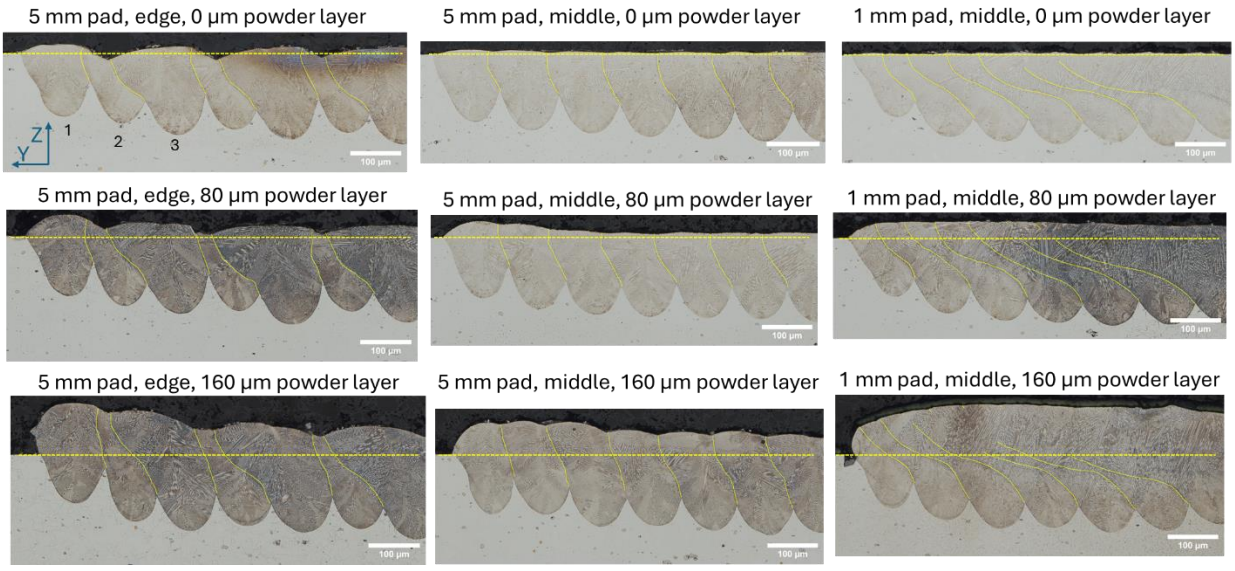

Figure 2. Montage of the melt pool cross-sections for different pad widths (5 mm or 1 mm), powder layer thicknesses (0 µm, 80 µm, 160 µm) and positions within each pad (5 mm edge = 0.460 mm, 5 mm middle = 2.545 mm, and 1 mm middle = 0.556 mm). Melt pool boundaries are traced for illustration. The approximate initial substrate surface is also drawn for illustration as the horizontal dashed line. The illustration lines are not measurements. Scale bars are 100 µm.

Table 2. Average melt pool bead height, depth, overlap depth, and width measurements. The standard deviation comes from 45 measurements per pad (44 for overlap depth) × 3 repeat pads. Here we note that "width" is a trailing half-width and should not be confused for the typical melt pool full width.

Powder Layer Thickness (µm)	Pad Size (mm)	Position (mm)	Avg. Bead Height (µm)	Std. Dev (µm)	Avg. Depth (µm)	Std. Dev (µm)	Avg. Overlap Depth (µm)	Std. Dev (µm)	Avg. Width (µm)	Std. Dev (µm)
0	5×5	0.460 (edge)	15.2	2.0	170.3	14.0	114.2	16.6	131.5	35.9
0	5×5	2.545 (middle)	6.0	1.1	175.6	11.2	121.0	13.9	115.9	11.0
0	1×5	0.556 (middle)	NA	NA	176.6	9.4	133.7	8.2	NA	NA
80	5×5	0.460 (edge)	23.9	7.7	164.0	15.6	106.2	15.2	130.4	41.3
80	5×5	2.545 (middle)	15.1	5.8	169.5	10.4	113.5	12.5	112.3	9.7
80	1×5	0.556 (middle)	NA	NA	168.4	9.6	124.0	8.7	NA	NA
160	5×5	0.460 (edge)	53.9	17.9	153.1	14.4	97.3	16.9	141.9	43.8
160	5×5	2.545 (middle)	43.0	8.5	159.2	11.1	104.8	12.9	117.0	10.2
160	1×5	0.556 (middle)	NA	NA	150.7	8.9	105.2	9.3	NA	NA

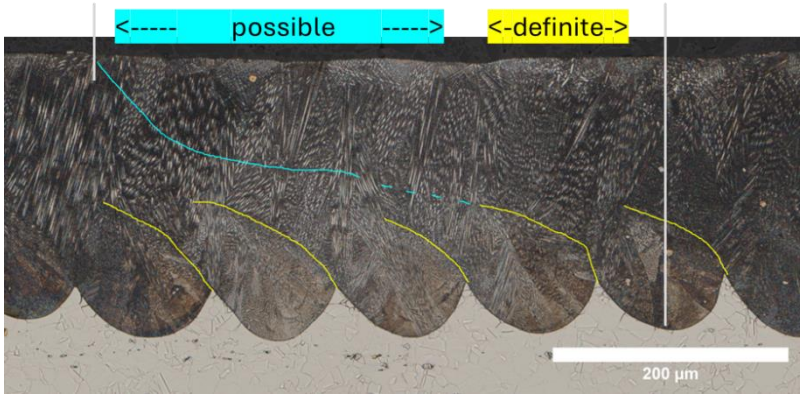

Figure 3. Example micrograph for 1 mm pad width with 0.75 ms turnaround time and 160 µm powder layer thickness illustrating the difficulty determining the melt pool boundary in the middle and near the top of the melted area. This resulted in "NA" for some bead height and width measurements. "Definite" is a clearly determined boundary. "Possible" is a best guess based on experience, but it was not considered measurable.

Modelers were also asked to compute the solidified area and dilution area (material above and below the initial substrate surface, respectively). This was measured using the Segment Anything model (https://doi.org/10.48550/arXiv.2304.02643) in MATLAB.

Occasionally, the segmentation result required some cleanup by hand. An example result for a portion of a pad is shown in Figure 4. The average results are provided in Table 3.

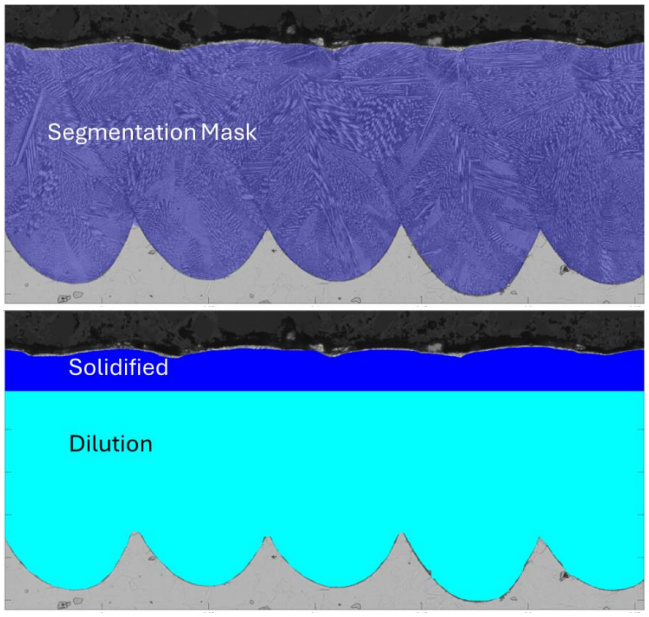

Figure 4. Image segmentation showing the masked melt pool (segmentation mask) over the grayscale of the original image and the division of the mask into the solidified and dilution layer areas based on the starting substrate surface.

Table 3. Average solidified and dilution layer areas. The standard deviation (std. dev.) comes from three repeats.

Powder Layer Thickness (µm)	Pad Size (mm)	Position (mm)	Solidified Layer Area (x 10^4 µm^2)	Std. Dev (x 10^4 µm^2)	Dilution Layer Area (x 10^4 µm^2)	Std. Dev (x 10^4 µm^2)
0	5×5	0.460 (edge)	4.83	0.68	76.52	0.87
0	5×5	2.545 (middle)	1.12	0.30	79.13	1.07
0	1×5	0.556 (middle)	0.13	0.16	79.44	0.61
80	5×5	0.460 (edge)	10.63	2.07	73.23	0.91
80	5×5	2.545 (middle)	5.60	1.40	75.72	0.91
80	1×5	0.556 (middle)	11.29	2.27	76.14	0.30
160	5×5	0.460 (edge)	26.01	2.00	67.82	0.74
160	5×5	2.545 (middle)	18.71	1.64	70.79	0.84
160	1×5	0.556 (middle)	36.65	2.80	66.99	0.35

Lastly, modelers were asked to provide the melt pool measurements for the first five tracks for the middle position of the 5 mm pad with 160 µm powder layer, see Table 4. Bead height and depth trends with track number for the full 45 tracks are also shown in Figure 5 for all three powder layer thicknesses showing how they decrease and increase, respectively, until reaching a flat trend with track number.

Table 4. Average melt pool bead height, depth, and width measurements. The standard deviation comes from 3 repeat pads. See the challenge and measurement description for definitions of melt pool measurements. Here we note that "width" is a trailing half-width and should not be confused for the typical melt pool full width.

Powder Layer Thickness (µm)	Pad Size (mm)	Position (mm)	Track No	Bead Height (µm)	Std. Dev (µm)	Depth (µm)	Std. Dev (µm)	Width (µm)	Std. Dev (µm)
160	5×5	2.545 (middle)	1	68.8	9.3	115.0	4.4	76.7	1.4
160	5×5	2.545 (middle)	2	68.2	9.2	127.9	7.7	92.5	6.1
160	5×5	2.545 (middle)	3	61.0	13.6	139.3	3.9	100.8	4.7
160	5×5	2.545 (middle)	4	54.5	14.9	139.5	4.4	102.2	1.8
160	5×5	2.545 (middle)	5	45.9	4.0	152.0	0.5	108.1	1.3

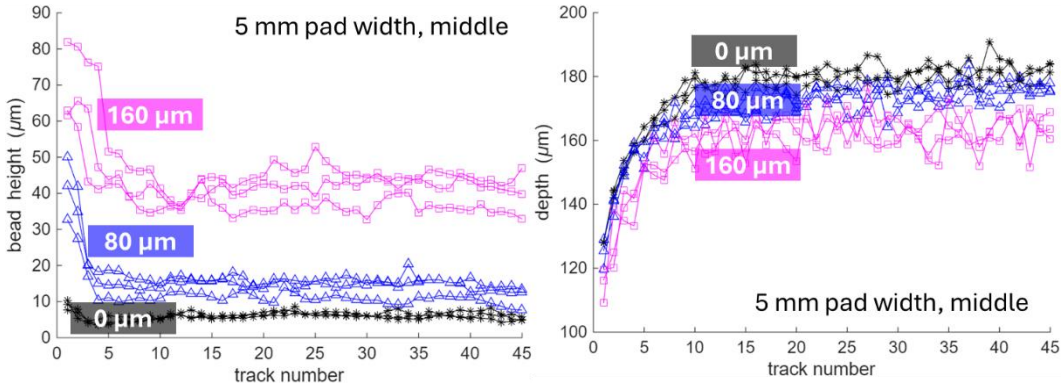

Figure 5. Melt pool bead height vs. track number and depth vs. track number for the three powder layer thicknesses. The pad width is 5 mm, location is middle (2.545 mm), and the laser turnaround time is 0.75 ms. Each powder layer thickness has three measurement series from the three repeats.

2.2 CHAL-AMB2025-06-PST

Modelers were asked to predict the root mean square height (Sq) and fused layer thickness for different areal and line profiles for the set of different pad widths and powder layer thicknesses. Representative surface height maps are shown in Figure 6 for layer thickness and Figure 7 for root mean square height. Additionally, height data for the 5 mm pad width

at 3 line profiles are given in Figure 8. The average and standard deviations are provided in Table 1.

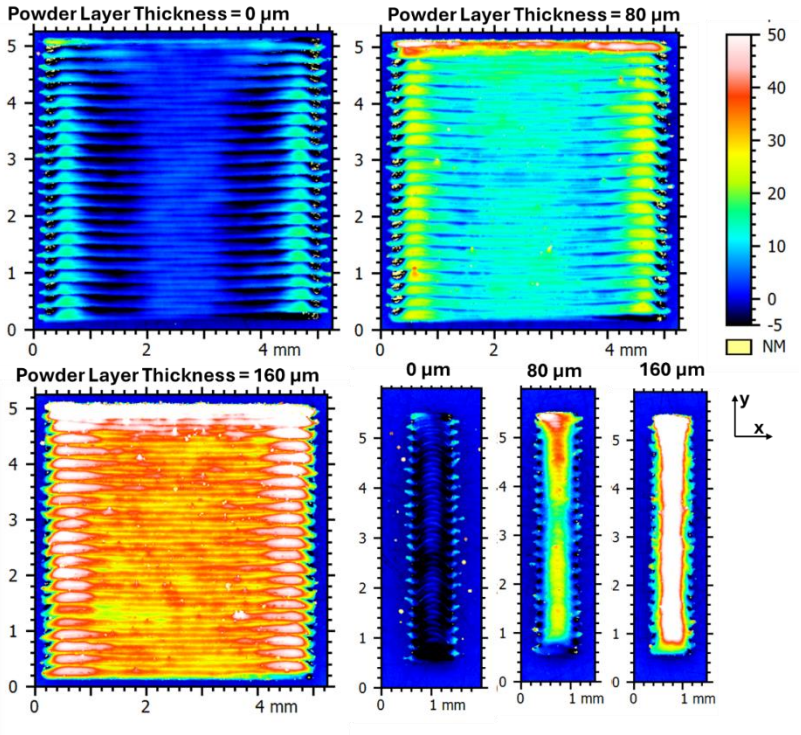

Figure 6. Representative surface height maps for different pad widths (5 mm and 1 mm) and powder layer thickness (0 µm, 80 µm, and 160) µm. The color scale is the same for all maps. Values larger than 50 µm are white.

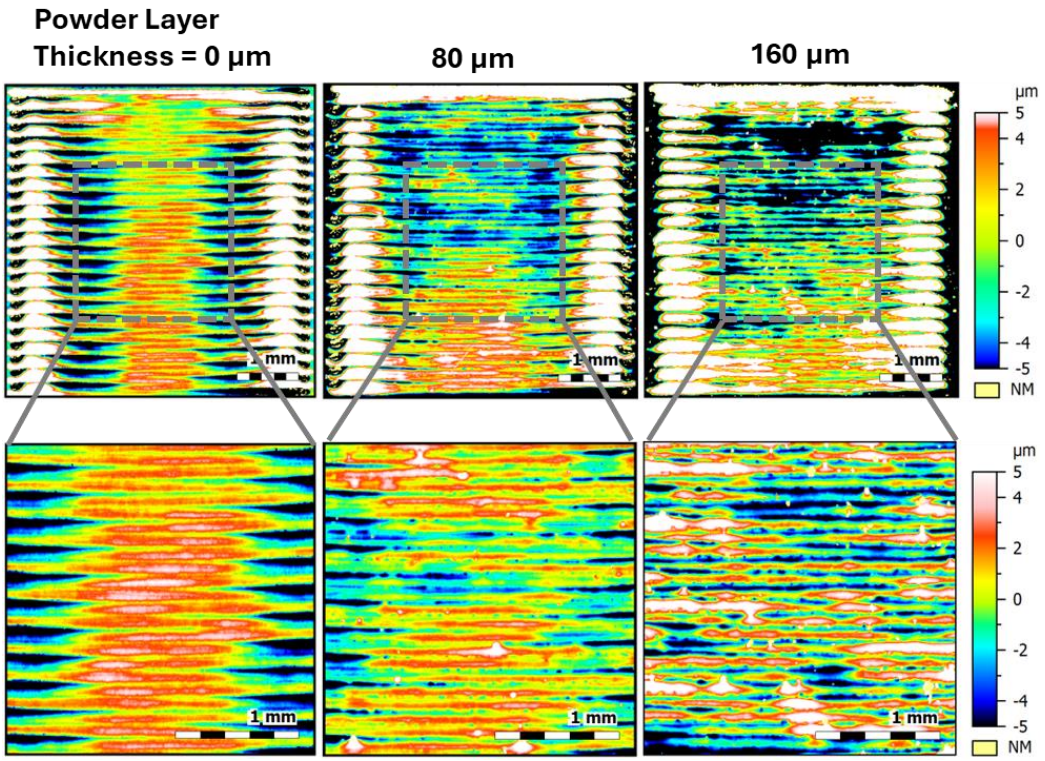

Figure 7. Surface height maps for root mean square height measurements for different powder layer thicknesses on the 5 mm wide pad.

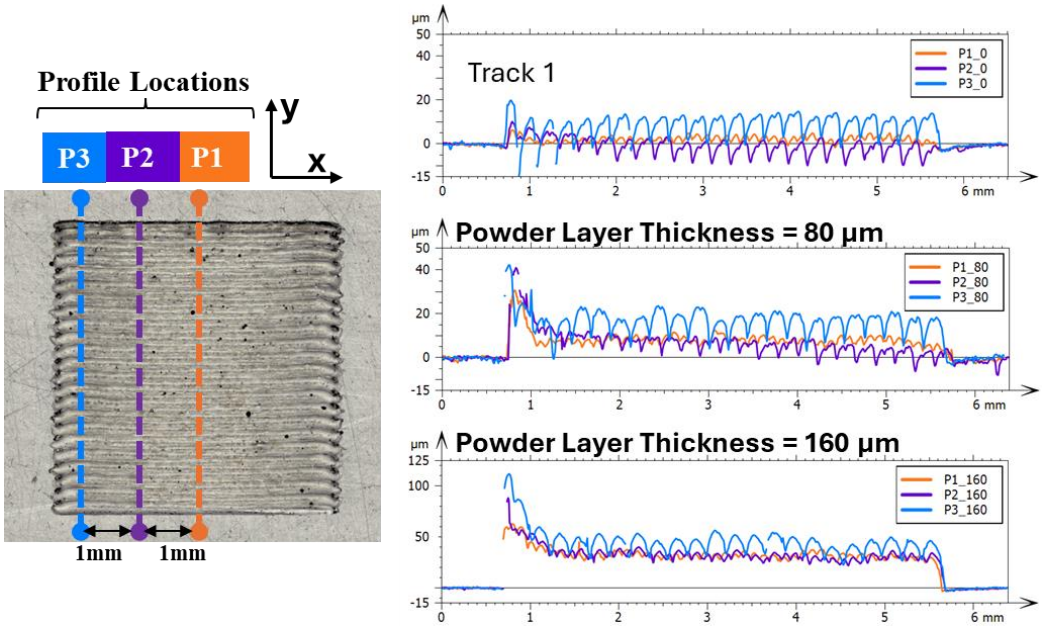

Figure 8. Surface height for line profiles P1, P2, and P3 in the 5 mm pad width for different powder layer thicknesses.

Table 5. Average and standard deviation measurement results for Sq and fused layer thickness for different pad widths and powder layer thickness at specific areal and line profiles.

Powder Layer Thickness (µm)	5 mm × 5 mm pad						1 mm × 5 mm pad	
	A1	A2	A3	P1	P2	P3	P4	A4
	Root mean square height (Sq) µm	Root mean square height (Sq) µm	Fused Layer Thickness (µm)	Fused Layer Thickness (µm)	Fused Layer Thickness (µm)	Fused Layer Thickness (µm)	Fused Layer Thickness (µm)	Fused Layer Thickness (µm)
0	8.46 ± 0.14	3.00 ± 0.07	0.99 ± 1.08	1.88 ± 0.39	-2.39 ± 1.05	11.20 ± 0.49	-1.57 ± 1.22	-1.03 ± 1.12
80	8.53 ± 1.03	2.30 ± 0.03	10.54 ± 1.49	11.15 ± 2.00	9.83 ± 1.80	22.45 ± 3.20	24.75 ± 3.21	17.83 ± 4.69
160	13.73 ± 0.44	3.77 ± 0.5	28.93 ± 0.22	35.61 ± 2.33	36.24 ± 3.16	49.88 ± 3.22	75.20 ± 5.42	72.98 ± 5.16

2.3 CHAL-AMB2025-07-PCRTAM

Modelers were asked to compute the mean, median, and standard deviation for the time above melt (TAM) and solid cooling rate (SCR) for a specific temperature range. Single line laser tracks were used to determine an average effective emissivity of 0.642 to convert radiant temperature to emissivity corrected temperature. The spatial maps and distributions for TAM and SCR are given in Figure 9 and Figure 10, respectively.

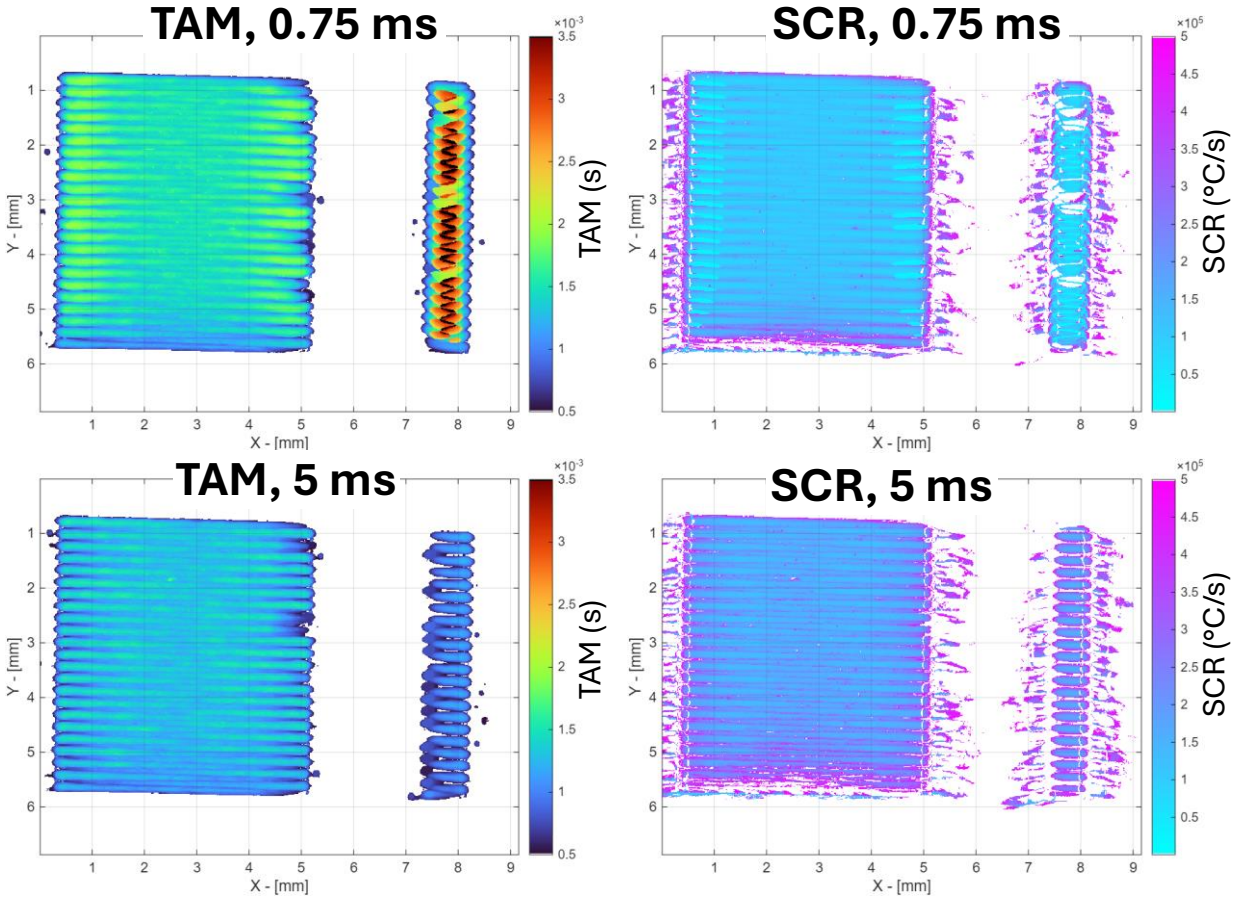

Figure 9. TAM and SCR maps for different pad widths (5 mm and 1 mm) and laser turnaround times (0.75 ms and 5 ms).

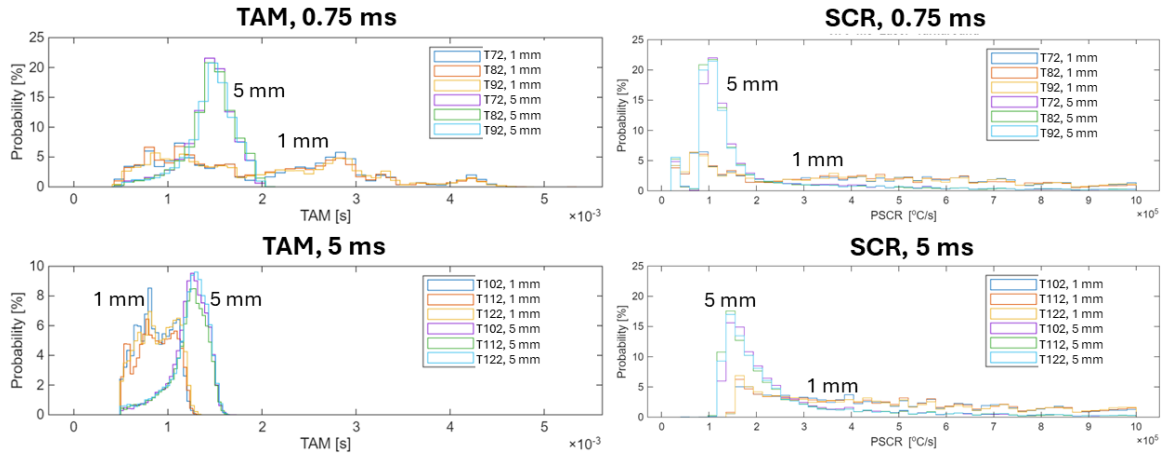

Figure 10. TAM and SCR distributions for different pad widths (5 mm and 1 mm) and laser turnaround times (0.75 ms and 5 ms).

TAM shows a fairly normal distribution that can be described by a mean and standard deviation, whereas SCR is non-normal and poorly described by a simple mean and standard deviation. Both TAM and SCR have artifacts from spatter and the vapor plume

that require conditioning. TAM values below 0.5 ms were ignored in the distribution. Spurious, high SCR values occurred around 10^7 °C/s, and values greater than 10^6 °C/s were ignored in the distribution. The distributions from the three repeats were combined to determine the aggregate mean, median, and standard deviation. TAM and SCR results are in Table 6 and Table 7, respectively.

Table 6. Mean, median, and standard deviation (std. dev.) time above melt (TAM) for bare plate (powder layer thickness = 0 µm) with different pad widths and laser turnaround times.

Sample Name	Pad Width (mm)	Turn-around time (ms)	N-datapoints [x 10^5]	TAM mean [x 10^{-3} s]	TAM median [x 10^{-3} s]	TAM std. dev. [x 10^{-3} s]
20241010_AMB_T72	1	0.75	2.18	2.00	1.80	1.00
20241010_AMB_T72	5	0.75	12.10	1.40	1.50	0.26
20241015_AMB_T82	1	0.75	2.21	1.90	1.70	0.99
20241015_AMB_T82	5	0.75	12.03	1.50	1.50	0.26
20241015_AMB_T92	1	0.75	2.21	2.00	1.80	1.00
20241015_AMB_T92	5	0.75	12.07	1.50	1.50	0.26
20241010_AMB_T102	1	5	2.00	0.86	0.85	0.19
20241010_AMB_T102	5	5	12.12	1.20	1.30	0.20
20241015_AMB_T112	1	5	1.99	0.87	0.87	0.20
20241015_AMB_T112	5	5	12.04	1.20	1.30	0.21
20241015_AMB_T122	1	5	1.96	0.89	0.89	0.20
20241015_AMB_T122	5	5	12.11	1.20	1.30	0.21
Aggregate	**1**	**0.75**	**6.59**	**2.00**	**1.80**	**1.00**
Aggregate	**1**	**5**	**5.95**	**0.87**	**0.87**	**0.20**
Aggregate	**5**	**0.75**	**36.20**	**1.50**	**1.50**	**0.26**
Aggregate	**5**	**5**	**36.27**	**1.20**	**1.30**	**0.21**

Table 7. Mean, median, and standard deviation (std. dev.) solid cooling rate (SCR) for bare plate (powder layer thickness = 0 µm) with different pad widths and laser turnaround times.

Sample Name	Pad Width (mm)	Turn-around time (ms)	N-datapoints [x 10^4]	PSCR mean [x 10^5 C/s]	PSCR median [x 10^5 C/s]	PSCR std. dev. [x 10^5 C/s]
20241010_AMB_T72	1	0.75	3.44	3.89	3.61	2.82
20241010_AMB_T72	5	0.75	13.33	1.96	1.23	1.82
20241015_AMB_T82	1	0.75	3.27	3.84	3.62	2.74
20241015_AMB_T82	5	0.75	13.13	1.92	1.19	1.85
20241015_AMB_T92	1	0.75	3.41	3.86	3.60	2.80
20241015_AMB_T92	5	0.75	13.30	1.96	1.20	1.87
20241010_AMB_T102	1	5	3.55	4.75	4.31	2.35
20241010_AMB_T102	5	5	13.50	2.70	1.99	1.77
20241015_AMB_T112	1	5	3.45	4.78	4.37	2.39
20241015_AMB_T112	5	5	13.41	2.63	1.90	1.79
20241015_AMB_T122	1	5	3.46	4.74	4.29	2.44
20241015_AMB_T122	5	5	13.47	2.68	1.93	1.83
Aggregate	**1**	**0.75**	**10.11**	**3.86**	**3.61**	**2.79**
Aggregate	**1**	**5**	**10.46**	**4.75**	**4.32**	**2.39**
Aggregate	**5**	**0.75**	**39.77**	**1.95**	**1.21**	**1.84**
Aggregate	**5**	**5**	**40.38**	**2.67**	**1.94**	**1.80**

2.4 CHAL-AMB2025-07-PMPG

Modelers were asked to predict the average melt pool bead height, depth, overlap depth, and width for the 45 tracks in pads at specific cross-section locations on bare plates for two different laser turnaround times (0.75 ms and 5 ms). Figure 11 shows representative micrographs for the first 7 tracks, and Table 8 provides the averages and standard deviations. Again, the bead height and width for the 1 mm pad with 0.75 ms turnaround time could not be reliably measured, which resulted in NA.

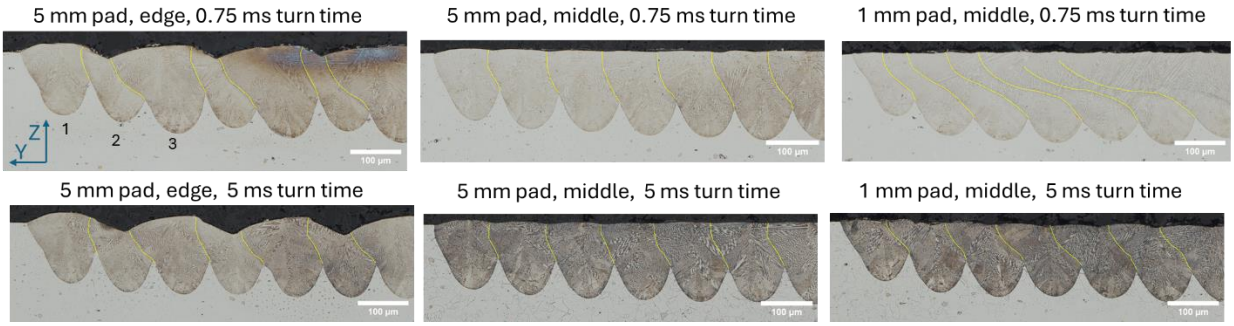

Figure 11. Montage of the melt pool cross-sections for different pad widths (5 mm or 1 mm) and laser turnaround time (0.75 ms or 5 ms). The powder layer thicknesses were 0 µm (i.e., bare plate). Melt pool boundaries are traced for illustration; this is not part of the measurement process. Scale bars are 100 µm.

Table 8. Average melt pool bead height, depth, overlap depth, and width measurements. The standard deviation comes from 45 measurements per pad (44 for overlap depth) × 3 repeat pads. See the challenge and measurement description for definitions of melt pool measurements. Here we note that "width" is a trailing half-width and should not be confused for the typical melt pool full width. The powder layer thickness was 0 µm (bare plate).

Laser Turn-around Time (ms)	Pad Size (mm)	Position (mm)	Avg. Bead Height (µm)	Std. Dev (µm)	Avg. Depth (µm)	Std. Dev (µm)	Avg. Overlap Depth (µm)	Std. Dev (µm)	Avg. Width (µm)	Std. Dev (µm)
0.75	5×5	0.460 (edge)	15.2	2.0	170.3	14.0	114.2	16.6	131.5	35.9
0.75	5×5	2.545 (middle)	6.0	1.1	175.6	11.2	121.0	13.9	115.9	11.0
0.75	1×5	0.556 (middle)	NA	NA	176.6	9.4	133.7	8.2	NA	NA
5	5×5	0.460 (edge)	14.9	2.5	149.7	6.4	85.2	8.4	102.3	12.6
5	5×5	2.545 (middle)	5.7	1.1	159.9	8.2	96.7	9.5	99.5	7.6
5	1×5	0.556 (middle)	-4.9	2.8	156.4	7.9	97.8	9.2	120.1	7.2

Lastly, modelers were also asked to provide a segmented image of the final melt pool (i.e., track number 45) for the six scenarios. Figure 12 shows the average mask with a red boundary for these six scenarios. Here we note that the melt pool boundary for 1mm, 0.75 ms is difficult to determine for reasons stated earlier, and this result is the best possible approximation.

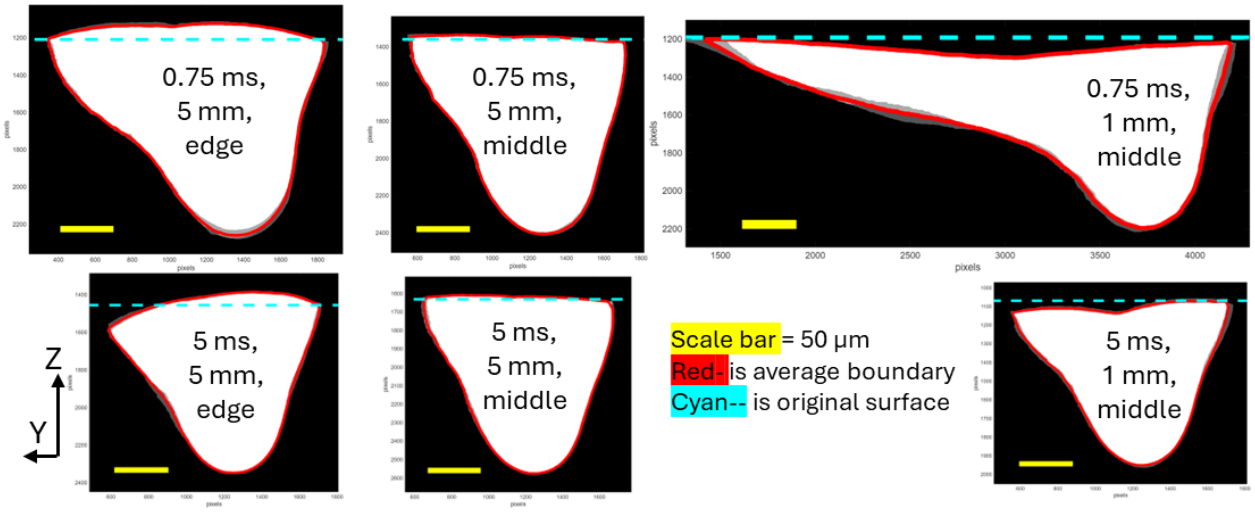

Figure 12. Montage of segmented melt pools for the last track (number 45) in pads for bare plate scans with different laser turnaround times (0.75 ms and 5 ms), different pad size widths (5 mm and 1 mm) and different locations within pads. The average boundary is from three repeats. The variation in the boundary is shown by the range between white and black (gray regions), which is approximately the same as the boundary line thickness for most images. The cyan dashed line is the original substrate surface.

3. Data Availability

Datasets will be made available as soon as possible. Please check back soon.

Available datasets can be found through the NIST AM-Bench website (https://www.nist.gov/ambench/am-bench-data-and-challenge-problems-0) and/or NIST Data Repository (https://data.nist.gov/).

4. References

Citations are provided throughout this document as hyperlinked URLs to the associated digital object identifier (DOI). Clicking these hyperlinked text should open the associated publication or cited source.

†Disclaimer The National Institute of Standards and Technology (NIST) uses its best efforts to deliver high-quality copies of the AM Bench database and to verify that the data contained therein have been selected on the basis of sound scientific judgment. However, NIST makes no warranties to that effect, and NIST shall not be liable for any damage that may result from errors or omissions in the AM Bench databases. Certain commercial equipment, instruments, or materials are identified in this paper in order to specify the experimental procedure adequately. Such identification is not intended to imply recommendation or endorsement by NIST, nor is it intended to imply that the materials or equipment identified are necessarily the best available for the purpose